NMR based metabolomics study of Y2 receptor activation by neuropeptide Y in the SK-N-BE2 human neuroblastoma cell line

ARTICLE *in* METABOLOMICS · FEBRUARY 2015

Impact Factor: 3.86 · DOI: 10.1007/s11306-015-0782-y

4 AUTHORS:

Bo Wang

University of Texas at Austin

13 PUBLICATIONS **111** CITATIONS

SEE PROFILE

Sulaiman Sheriff

University of Cincinnati

80 PUBLICATIONS **1,425** CITATIONS

SEE PROFILE

Ambikaipakan Balasubramaniam

University of Cincinnati

170 PUBLICATIONS **3,511** CITATIONS

SEE PROFILE

Michael A Kennedy

Miami University

158 PUBLICATIONS **3,451** CITATIONS

SEE PROFILE

NMR based metabolomics study of Y2 receptor activation by neuropeptide Y in the SK-N-BE2 human neuroblastoma cell line

Bo Wang, Sulaiman Sheriff, Ambikaipakan Balasubramaniam & Michael A. Kennedy

Metabolomics
An Official Journal of the Metabolomics Society

ISSN 1573-3882

Metabolomics
DOI 10.1007/s11306-015-0782-y

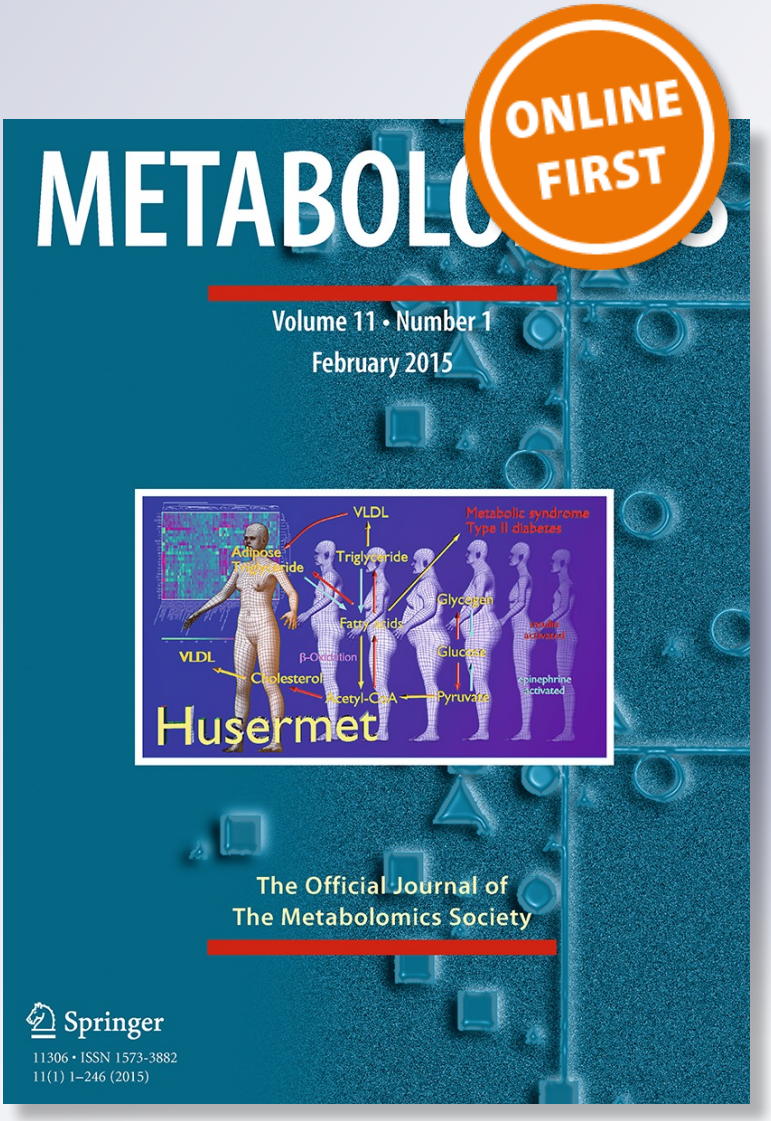

Springer

Metabolomics
DOI 10.1007/s11306-015-0782-y

ORIGINAL ARTICLE

NMR based metabolomics study of Y2 receptor activation by neuropeptide Y in the SK-N-BE2 human neuroblastoma cell line

Bo Wang · Sulaiman Sheriff · Ambikaipakan Balasubramaniam · Michael A. Kennedy

Received: 4 August 2014 / Accepted: 27 January 2015

Abstract Neuropeptide Y (NPY) and its Y2 receptors (Y2R) play an important role in regulating growth of various tumors and are highly expressed in human neuroblastoma brain tumors. Cell lines derived from neuroblastoma brain tumors provide a good model to study the consequences of NPY activation of Y2R in tumor metabolism. In this study, the metabolic response to activation and inhibition of Y2R was examined in the human neuroblastoma cell line SK-N-BE2 using high-resolution nuclear magnetic resonance spectroscopy (NMR). Three treatments were evaluated: (1) activation of Y2R with NPY, (2) blocking Y2R with BIIE0246, and (3) treatment of cells with both NPY and BIIE. The largest metabolic changes were observed for NPY activation of Y2R. The principal response to NPY activation of Y2R was increased glycolysis (Warburg effect). Our results also showed depleted intracellular nutrients in NPY activated cells, which may have been due to the high rate of conversion of glucose to lactate, glycine and alanine. All amino acids except glutamine were increased in response to Y2R activation, implying increased autophagic degradation of proteins. TCA cycle intermediates were not detected, possibly due to low steady-state concentrations, but the increase of glutamate and its high correlation with glucose provided evidence of increased TCA activity. The changes of most metabolites observed upon NPY treatment were reversed with BIIE treatment. In summary, our study indicates that NPY activation of Y2R in human neuroblastoma cells stimulates glycolysis, glutaminolysis and possibly TCA activity.

Keywords NMR · Metabolomics · Metabonomics · Neuropeptide Y · Y2 receptor · Neuroblastoma · Cancer · Brain tumor · BIIE0246 · SK-N-BE2

1 Introduction

Neuropeptide Y (NPY) is a 36 amino acid peptide initially reported as being abundant in brain tissue (Chronwall and Zukowska 2004; O'Donohue et al. 1985; Tatemoto et al. 1982) and since understood to be expressed and strictly localized in neurons (Gehlert 2004). NPY is ubiquitous in both the peripheral and central nervous systems (Ingenhoven and Beck-Sickinger 1999) where it acts both as a neurotransmitter and a neuromodulator (Smialowska et al. 2009). NPY exerts neuroendocrine action that serves to regulate several physiological processes including blood pressure, appetite, brain seizures, anxiety, bone formation, Luteinizing hormone secretion, pain sensitivity, depression, gastrointestinal motility, angiogenesis and ethanol consumption (Gehlert 2004). Because of its relationship to many human physiological processes, the NPY system has been considered as a therapeutic target (Brothers and Wahlestedt 2010; Eaton et al. 2007; Zhang et al. 2011). NPY has also been identified as a pro-oncogenic factor for neuroblastomas, breast and prostate cancers (Brothers and

Electronic supplementary material The online version of this article (doi:10.1007/s11306-015-0782-y) contains supplementary material, which is available to authorized users.

B. Wang · M. A. Kennedy (✉)
106 Hughes Laboratories, Department of Chemistry and Biochemistry, Miami University, 651 East High Street, Oxford, OH 45056, USA
e-mail: kennedm4@miamioh.edu

S. Sheriff · A. Balasubramaniam
Department of Surgery, University of Cincinnati Medical Center, Cincinnati, OH 45267, USA

Published online: 06 February 2015

Wahlestedt 2010). NPY acts through binding several identified G-protein coupled receptors (Y1-, Y2-, Y4-, Y5-, and Y6-R), which have been reported to be involved in cell proliferation (Hansel et al. 2001), matrix invasion and metastasis in different types of cancers (Ruscica et al. 2007). Among these receptors, Y1R, Y2R and Y5R induce endothelial cell migration (Movafagh et al. 2006).

Y1 and Y2 receptors have been implicated in breast carcinomas, adrenal gland, renal cell carcinomas, and ovarian cancers according to a recent review (Korner and Reubi 2007). Cell proliferation activated by Y1R and Y2R was reported in a study of vascular smooth muscle cells (Erlinge et al. 1994), neural crest tumors (Kitlinska et al. 2005), breast cancer cell lines (Medeiros et al. 2012; Reubi et al. 2001) and neuroblastoma cell lines (Lu et al. 2010). NPY Y5 receptor has been reported to increase cell growth and migration in human breast cancer cells (Medeiros et al. 2012; Medeiros and Jackson 2013; Sheriff et al. 2010). Y2R is found in both tumor and normal cells (Lu et al. 2010; Reubi et al. 2001), and Y2R activation increases angiogenesis (Lee et al. 2003; Ruscica et al. 2007) and satiety (Acosta et al. 2011; Zhang et al. 2011). High Y2R expression is found in human brain tumors such as neuroblastomas (Kitlinska et al. 2005; Korner and Reubi 2008; Korner et al. 2004) and glioblastomas (Korner and Reubi 2008). The proliferation of neuroblastoma cells was found to be related with NPY by the activation of Y2/Y5Rs (Kitlinska et al. 2005), and Y2R was considered as a potential target of neuroblastoma therapy (Lu et al. 2010).

Selective antagonists for Y1R, Y2R, Y4R and Y5R have been studied to understand the physiological properties of NPY and its receptors (Cabrele and Beck-Sickinger 2000). Y2R antagonist, JNJ-31020028, was investigated for nicotine abstinence-related behavior (Aydin et al. 2011), and Y2R antagonist BIIE0246 was found effectively to inhibit growth of neuroblastoma cells (Kitlinska et al. 2005; Lu et al. 2010). Y2R antagonists provide tools to selectively study the metabolic consequences of activation of Y2R by NPY. In addition, many antagonists have been found to cross the blood–brain barrier making them suitable for pharmacological study (Brothers et al. 2010).

While the association between Y2R and neuroblastoma cell proliferation has been established, and the Y2R has been found highly expressed in brain tumors and considered as a potential target for treatment, the metabolic response to activation of Y2R by NPY in neuroblastoma cells has not been well studied. In this paper, we used high-resolution nuclear magnetic resonance spectroscopy (NMR) to investigate the metabolic consequences of Y2R activation by NPY in human neuroblastoma SK-N-BE2 cells and the influence of selectively blocking Y2R with the BIIE0246 antagonist (BIIE).

2 Materials and methods

2.1 Numbers of samples

Six biological replicates were prepared for each group consider in this study and described below.

2.2 Cell culture

The human neuroblastoma cell line SK-N-BE2 was used in this study. The neuroblastoma cells were grown in Eagle's essential medium (EMEM), supplemented with 10 % fetal calf serum (FBS), penicillin (100 IU/mL) and streptomycin (100 μg/mL) in a 95 % air/5 % CO_2 humidified atmosphere at 37 °C as reported previously (Balasubramaniam et al. 2000). When the cells became 90 % confluent (4–5 days), medium was replaced with the EMEM containing 0.25 % FBS, and was used in the treatment experiments described below.

2.3 Cell line treatments

Three treatments were studied. *Group 1* compared NPY-treated cells to a control (water) to monitor the cellular response to activation of Y2R by NPY. In *Group 2*, the Y2R receptor was blocked by BIIE (dissolved in ethanol) in treated cells and compared to cells treated with neat ethanol as a control. In *Group 3*, cells were treated with BIIE plus NPY versus NPY treatment alone to study the effect of selective blocking of Y2R in this Y2R-rich cell line. The dose concentration of NPY 100 nM and BIIE0246 was 1 μM. The dose values were chosen based on published values shown to activate and inhibit NPY Y2R, respectively, in different tissue/cell systems (Dumont et al. 2000; Kitlinska et al. 2005). The SK-N-BE2 cells were treated with 1 μM Y2R antagonist, BIIE0246 in 0.25 % FBS containing DMEM media. Fifteen minutes later 100 nM NPY was added to the cells and the incubation continued for additional 24 h and the media and the cells were extracted for the analysis. The order of treatment was antagonist first, 15 min later the agonist was added. NPY treatment for 48 h has been shown to increase cell growth by 40 % and this increase was blocked by BIIE0246 (Kitlinska et al. 2005). The relative affinity of NPY (agonist) for Y2R is 0.2 nM and BIIE0246 (antagonist) is 15 nM (Dumont et al. 2000).

2.4 Harvesting of cells and spent media

When cells were grown to 75–85 % confluence in 10 cm culture dishes, the media was aspirated and cells were trypsinized using trypsin–EDTA solution (Invitrogen). Fresh growth media containing 10 % FBS was added to the

trypsinized cells (10:1 ratio) and centrifuged for 5 min at 1,500 rpm at 4 °C. The spent media was aspirated and stored for analysis and the cell pellet was washed with 10 mL of cold phosphate buffered saline, pH 7.4, and centrifuged again as above. This step was repeated two more times and the cell pellets were stored at −80 °C until removal for cell extraction.

2.5 Cell extraction

Intracellular metabolites were analyzed following extraction using the methanol-chloroform-water method as previously described (Gottschalk et al. 2008; Watanabe et al. 2012). Briefly, the cell pellets were resuspended an ice-cold methanol and chloroform solution with a ratio of 2:1. The same total volume of ice-cold water and chloroform (1:1) was added after resuspension. The hydrophilic extraction was obtained by taking the top layer of the mixture after sonication and centrifugation, and the samples were dried in a SpeedVac centrifuge for about 2–3 h before storing in −20 °C until prepared for NMR analysis.

2.6 NMR spectroscopy

NMR spectra were collected using a 600 MHz Bruker Avance III NMR spectrometer. Data were recorded at 298 K using 3 mm NMR tubes (Norell) with a spectral width of 17 ppm. Two ^{1}H NMR experiments optimized were run on all samples: a standard 1D pulse and acquire pulse sequence employing water-suppression using pre-saturation (zgpr) and the one-dimensional first increment of a nuclear Overhauser effect spectroscopy (NOESY) experiment with pre-saturation (noesygppr1d). FIDs were apodized using exponential multiplication (EM) with line broadening equal to 0.3 Hz prior to Fourier transformation. A typical NMR spectrum is shown in Fig. S1. All experiments included on-resonance water pre-saturation achieved by irradiation during a 4.0 s relaxation delay. The 90° pulse width was determined for every sample using the automatic pulse calculation feature in TopSpin 3.1 (Wu and Otting 2005). All pulse widths were 8.5 ± 0.5 µs. The zgpr experiment was used to screen samples and ensure that pre-saturation and shimming were sufficient to collect reliable data. Shimming quality was determined by measuring the full width at half height (FWHH) of the Trimethylsilyl propionate (TSP) peak, which was deemed acceptable when the FWHH <1.0 Hz. One-dimensional zgpr ^{1}H spectra were acquired using 8 scans and 2 dummy scans, with 45 K points per spectrum. This resulted in an acquisition time of 1.92 s. Once the spectrum was determined to be of acceptable quality the 1D NOESY experiment was collected. The one-dimensional first increment of the NOESY experiment was collected using 128 scans with 4 dummy scans. 65 K points per spectrum were collected which resulted in an acquisition time of 3.21 s. All NMR spectra were processed using the AU program apk0.noe. This AU program automatically corrects phase, baseline, and chemical shift registration relative to TSP in TopSpin 3.1.

2.7 Principal component analysis (PCA) and statistical significance analysis

NMR spectra bucketing and PCA were conducted using Amix (Bruker Biospin, Billerica, MA, USA). Dynamic manual bucketing enabled use of unequal bucket widths, which allowed for optimization of the bucket widths and the center frequency of the buckets to ensure that a single peak was included in one bucket. Consequently, the manual bucketing guaranteed that the bucket intensity accurately preserve metabolite concentration information (Lindon et al. 2007). Prior to manual bucketing, spectral were aligned relative to the added TSP. After alignment, buckets belonging to the same metabolite and the same peak feature were determined manually as well. Any spectral features that were obviously overlapped based on visual inspection were excluded from the analysis. All spectra were subjected to *total intensity normalization* (Zhang et al. 2009) and *Pareto scaling* (van den Berg et al. 2006) was applied before PCA. Residual water and internal standard peaks were excluded from analysis. Statistical significance analysis of the loadings data was performed using Amix based on the procedure we have previously published (Goodpaster et al. 2010) except that a Kruskal–Wallis test (Kruskal and Wallis 1952) was used instead of the Mann–Whitney *U* test for non-parametric analysis of datasets that were not normally distributed.

2.8 Metabolite identification

Metabolites were putatively identified at MSI level 2 using the Chenomx NMR suit (Chenomx Inc. Edmonton, Alberta, Canada). The assigned peaks for the metabolites are listed in Table S1. The Pearson correlation coefficients were calculated to assess correlated changes in metabolite concentrations (Tables S2 and S3) using Matlab R2012a (Mathworks, MA, US).

3 Results and discussion

3.1 NMR spectra analysis of hydrophilic extracts and spent media

A total of 23 metabolites were identified from more than 80 non-overlapped peaks, which were then subjected to

statistical significance analysis. The annotated metabolites are listed in Table S1.

3.2 PCA and statistical analysis

Unsupervised PCA was applied to each group to analyze sample clustering. For the NPY-treated cells, statistically significant group separation was observed in the scores plot for the first two principal components (PCs) based on measurement of the Mahalanobis distance between groups (Goodpaster and Kennedy 2011) (Fig. 1a) implying statistically significant differences in the concentrations of intracellular concentrations of metabolites. The loadings plot (Fig. 1b) shows the contribution that each variable (NMR peak) made to the clustering and separation observed in the scores plot. Variables that deviate from the origin in the same direction as the separation observed in the scores plot are potentially important (Zhang et al. 2009). From the loadings plot (Fig. 1b), we can see that the intracellular concentrations of glucose, pyruvate and glutamine were lower in NPY-treated cells, but many amino acids and *O*-phosphocholine were more concentrated in NPY-treated samples. In the BIIE-treated cells (Fig. S2), the separation was mainly along PC2. Glucose was higher in the control and lactate was higher in the Y2R blocked cells but the changes were not statistically significant (Table 1). This is not surprising since the Y2R is not being actively stimulated in the absence of added NPY so blocking of the inactivated Y2R with BIIE has little consequence. In the NPY+BIIE-treated cells (Fig. 2), the separation direction was similar to that observed for the NPY-treated cells, but glucose was more concentrated in NPY-treated cells whereas lactate and acetate were more concentrated in the BIIE+NPY-treated group. Changes in metabolite concentrations between groups were assessed for statistical significance by calculating the p values for the intensity distributions of individual metabolite peaks and comparing the calculated p values to the critical p values computed using two different p value correction methods including the Bonferroni correction (BC) (Simes 1986), and Standard deviation step down (SDSD) (Wang et al. 2013). The statistical significance analysis of the concentration changes and fold-changes for the metabolites are listed in Table 1.

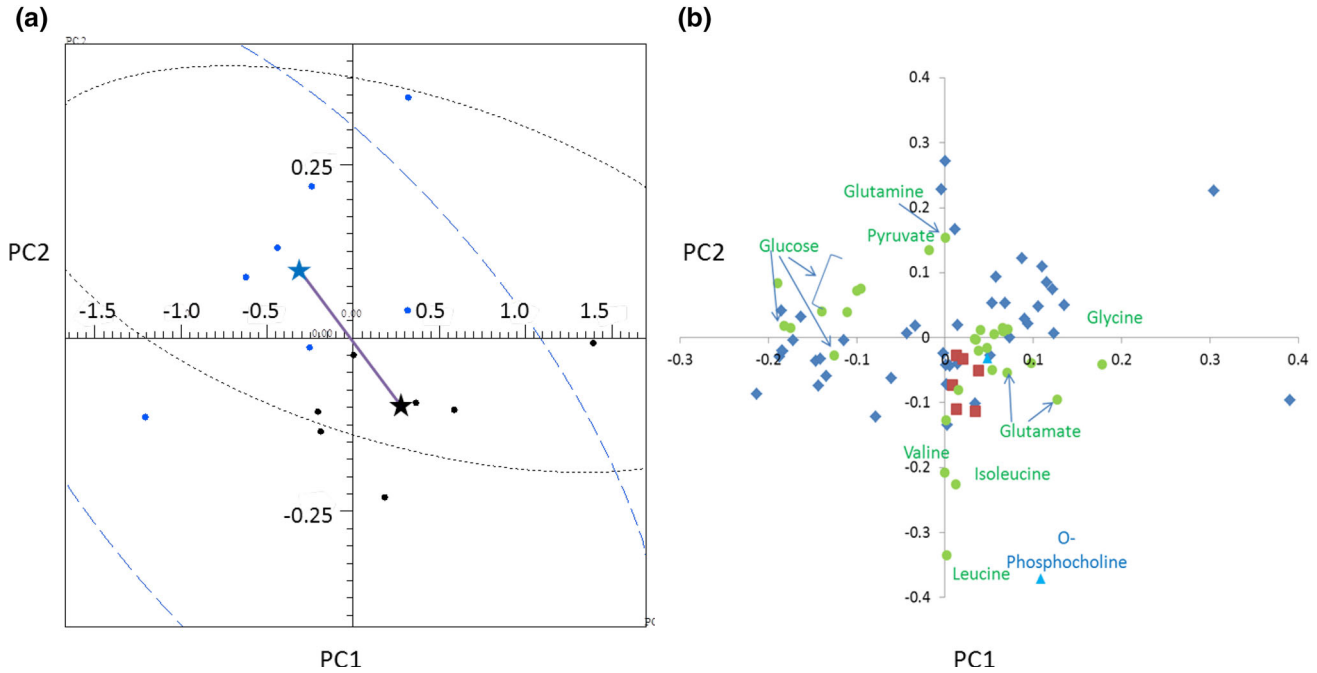

Fig. 1 The PCA scores and loadings plot for NPY-treated cells versus the control. **a** In the scores plot, the *black dots* represent the NPY-treated cells and *blue dots* are the control group. A *star* marks the center of each group in the scores plot and a *line* connecting the *stars* indicates the direction between the groups. The Mahalanobis distance between groups is 2.93 with F value of 13.8. The first two PCs accounted for 90 % of the variance between groups. The 95 % confidence intervals for the distribution of scores for each group are represented by the *dotted* (*black*) and *dashed* (*blue*) *ellipses*. **b** In the loadings plot, the *points* are colored according to their *p* values and statistical significance in the following way *red squares* ($p <$ BC), *light blue triangles* ($p <$ SDSD), *green dots* ($p < 0.05$) and *dark blue diamonds* ($p > 0.05$) (Color figure online)

Table 1 Cell line extracts metabolites with p values smaller than 0.05 in at least one group-wise comparison

Metabolites	ppm	Group 1		Group 2		Group 3	
		p value	Fold change	*p* value	Fold change	*p* value	Fold change
Acetate	1.92	2.10E-01	1.03	1.42E-01	1.09	1.75E-03	−1.25***
Alanine	1.48	1.47E-01	1.07	2.25E-01	−1.06	5.53E-03	−1.14**
Aspartate	2.70	4.21e-02*	1.07	3.50e-02*	1.13	1.33E-03	1.17***
	2.80	1.01e-02*	1.10	1.81e-02*	1.13	8.16E-04	1.19***
Glucose	3.25	4.33e-02*	−1.10	1.10E-01	1.09	6.01E-03	1.24*
	3.27	3.51e-02*	−1.06	4.76e-02*	1.09	1.38E-03	1.17***
	3.39	3.61e-02*	−1.10	3.38E-01	1.05	2.78E-03	1.26**
	3.40	3.08e-02*	−1.10	2.77E-01	1.07	3.60E-03	1.26**
Glutamate	2.33	4.76e-02*	1.08	4.76e-02*	−1.07	5.85E-02	−1.10
	2.36	1.81e-02*	1.10	4.82E-01	−1.03	2.53E-02	−1.13*
	2.37	6.01e-03*	1.12	3.38E-01	1.02	2.58E-02	−1.14*
Glutamine	2.45	1.10E-01	−1.04	6.55E-01	−1.00	6.65E-04	1.09***
	2.48	3.27e-02*	−1.04	3.38E-01	1.02	4.04E-03	1.07**
Glycine	3.56	1.50E-02	1.11	4.82E-01	1.00	1.10E-01	−1.06
Isoleucine	0.94	1.84e-04***	1.04	6.55E-01	−1.00	1.68E-03	1.04***
	1.02	8.81E-03	1.03	1.42E-01	1.02	8.95E-02	1.01
Lactate	1.33	1.80E-01	1.06	4.32e-02*	−1.18	2.68E-03	−1.32**
	4.10	4.45E-01	1.03	1.39e-02*	−1.21	8.63E-04	−1.29***
	4.11	3.82E-01	1.03	3.47e-02*	−1.18	4.30E-04	−1.33***
Leucine	0.97	1.15e-02*	1.03	8.45E-02	1.02	4.51E-03	1.03**
O-Phosphocholine	3.21	9.89e-03**	1.11	1.80E-01	1.07	5.16E-01	−1.03
Pantothenate	0.90	3.48e-02*	1.07	1.10E-01	1.06	5.71E-01	1.02
Phenylalanine	7.34	3.69e-03*	1.04	2.53e-02*	1.06	4.24E-01	1.01
	7.43	5.88e-03*	1.06	1.10E-01	1.04	8.45E-02	1.01
Proline	3.35	3.64e-02*	1.09	4.82E-01	1.02	3.04E-01	−1.04
Pyroglutamate	4.18	2.58e-02*	1.06	2.77E-01	1.03	1.27E-02	−1.06*
	4.19	5.73E-02	1.04	3.50e-02*	1.11	9.10E-01	1.00
Pyruvate	2.38	2.19e-02*	−1.36	5.08E-02	1.18	2.67E-02	1.15*
Sn-glycero-3-phosphocholine	3.23	9.80E-02	1.12	1.45e-02*	−1.22	1.81E-02	−1.18*
Threonine	4.24	2.22e-04***	1.13	1.80E-01	1.05	1.33E-01	−1.05
	4.25	3.59e-03**	1.08	2.77E-01	1.04	2.20E-01	−1.03
Tyrosine	6.90	9.48e-04***	1.04	1.10E-01	−1.03	7.25E-01	−1.00
	6.91	7.69e-04***	1.05	4.06E-01	1.02	1.15E-01	−1.02
Valine	0.99	2.77e-02*	1.02	2.25E-01	1.00	4.09E-03	1.02**
	1.05	1.80E-01	1.02	2.25E-01	−1.01	5.87E-02	1.01

Fold change indicates the ratio of the treatment group means to the control group means. A negative fold change indicates that the treated group has a lower average metabolite concentration compared to the control group

*** $p <$ BC, ** $p <$ SDSD and * $p < 0.05$

3.3 Biological significance of metabolite changes

3.3.1 Glycolysis

Most cancer cells exhibit elevated glycolysis, i.e. a Warburg effect (Bensinger and Christofk 2012), which means that glucose conversion to lactate is a preferred process of energy production for the cells even in an oxygen-abundant environment. Since glucose was a dominant factor in determining the direction of separation in the scores plots in NPY-treated cells and NPY+BIIE-treated cells, the metabolites involved in glycolysis are analyzed in detail in this section. The depletion of intracellular glucose following NPY activation of Y2R (*Group 1*) was consistent

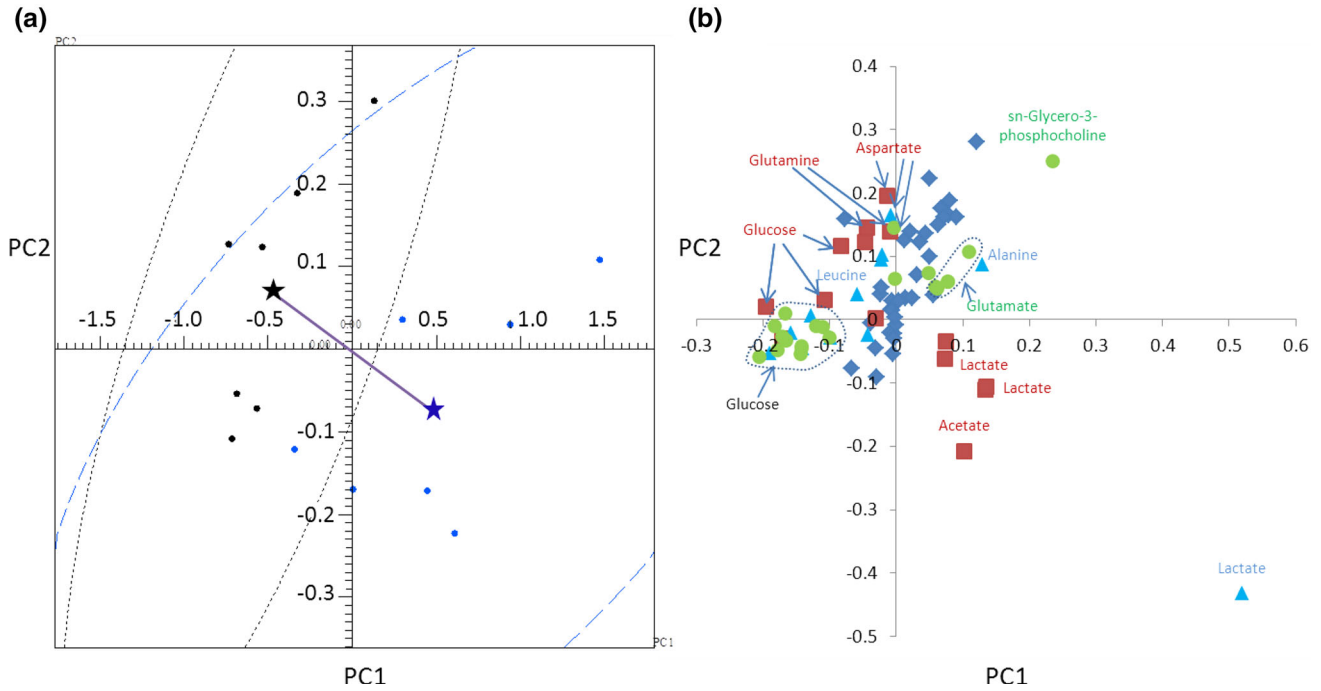

Fig. 2 The PCA scores and loadings plot for NPY+BIIE-treated cells compared with the control group. **a** In the scores plot, *black dots* represent NPY+BIIE-treated cells and *blue dots* represent the NPY-treated control group. A *star* marks the center of each group in the scores plot and a *line* connecting the *stars* indicates the direction between the groups. The Mahalanobis distance between groups is 3.58 with an F value of 20.54. The first two PCs accounted for 95 % of the variance between groups. The 95 % confidence intervals for the distribution of scores for each group are represented by the *dotted* (*black*) and *dashed* (*blue*) *ellipses*. **b** In the loadings plot, the *points* are colored according to their *p* values and statistical significance in the following way *red squares* ($p <$ BC), *light blue triangles* ($p <$ SDSD), *green dots* ($p < 0.05$) and *dark blue diamonds* ($p > 0.05$) (Color figure online)

with increased glycolysis, since glycolysis consumes intracellular glucose. The decreased intracellular concentrations of glutamine and pyruvate imply activation of the TCA cycle since pyruvate is consumed by TCA cycle activity and glutamine is used as an additional energy source that feeds into the TCA cycle through the process of glutaminolysis. The trends for the changes in glucose and glutamine concentrations were reversed with NPY+BIIE treatment (*Group 3*) and the intracellular aspartate concentration was also increased. These changes indicate suppressed glycolysis and reduced TCA cycle activity, indicated by the lower concentration of intracellular aspartate, which is a product of TCA cycle activity. The changes in intracellular glucose concentrations were strongly negatively correlated with changes in intracellular lactate concentrations in both *Group 1* ($r = -0.96$, Table S2) and *Group 3* ($r = -0.97$, Table S3), which further supported the conclusion that glucose conversion to lactate was associated with stimulation of glycolysis.

In addition to cell extracts, we also measured glucose and lactate levels in the spent media. Glucose provides an energy source for the cells and lactate produced by glycolysis in the cells will accumulate in the spent media. Consequently, it is very useful to analyze the spent media to monitor glycolysis activity. The changes in the concentrations of lactate and glucose in the spent media for all three groups are listed in Table 2. For *Group 1*, glucose in the media was significantly decreased after activation of Y2R with NPY while lactate level in the media was significantly increased. Since glucose was initially present in the media but lactate was not, this indicates that NPY activation of Y2R stimulated glycolysis, consumption of glucose from the media, and the Warburg effect. After the BIIE was added to block the Y2R receptor (*Group 2*), the glucose levels were higher in the spent media and lactate levels lower compared to the control, indicating mild but statistically insignificant suppression of glycolysis. When BIIE was added to the cells in addition to NPY (*Group 3*), the glucose level in the media remained high and the lactate level dropped even lower than with BIIE alone, indicating that the Y2R was strongly and effectively suppressed by BIIE even in the presence of added NPY.

The diagram in Fig. 3 summarizes the overall changes observed in glycolysis. The high glucose consumption associated with NPY activation of Y2R leads to lower intracellular glucose concentrations and significant decreases in the spent media. Glucose conversion to lactate was increased in NPY-treated cells as indicated by accumulation

Table 2 Glucose and lactate concentration changes in the spent media

Metabolites	ppm	Group 1		Group 2		Group 3	
		p value	Fold change	*p* value	Fold change	*p* value	Fold change
Glucose	3.25	1.11E-04	−1.05	3.41E-06	1.04	4.85E-06	1.04
	3.90	8.63E-07	−1.05	1.24E-05	1.04	1.47E-06	1.04
Lactate	1.34	1.75E-03	1.20	4.25E-07	−1.28	9.17E-08	−1.34
	4.12	7.02E-06	1.28	9.90E-05	−1.21	2.19E-07	−1.34

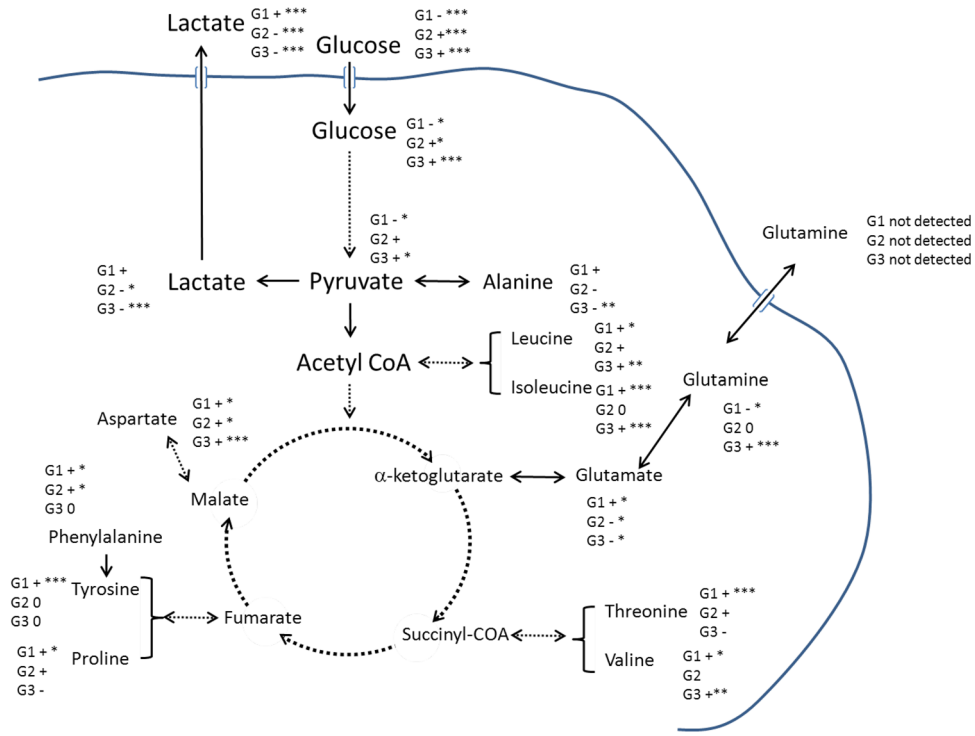

Fig. 3 Summary of changes for glucose, lactate, pyruvate and amino acids. G1 represents NPY-treated cells. G2 represents BIIE-treated cells, and G3 represents NPY+BIIE-treated cells. + means that the treated group has a higher average concentration than the control for this group and − means that the treated group has a lower average concentration. *$p < 0.05$, **$p <$ SDSD correction, ***$p <$ BC. The *solid blue line* separates determination of intracellular metabolites from metabolites measured in the spent media (Color figure online)

of lactate in the media. Lower pyruvate levels and higher alanine levels were also observed in NPY-treated cells. Since the conversion of pyruvate to lactate and alanine has been detected in brain tumors (Maher et al. 2012; Park et al. 2010), increased conversion of pyruvate to lactate and alanine has been suggested to indicate high dependence on anaerobic breakdown of pyruvate in cancer cells and the accumulation of intracellular lactate may create cellular conditions that promote cancer cell proliferation (Hirayama et al. 2009).

3.3.2 Amino acids

Intracellular concentrations of alanine, glutamate, glycine, proline, threonine, tyrosine, and valine were increased after activation of Y2R with NPY. Increased concentrations of amino acids have also been observed in colon and stomach tumors compared to normal cells in a mass spectrometry study (Hirayama et al. 2009). Our study indicates that the NPY activation of Y2R leads to increased intracellular concentrations of amino acids that support the growth of cancer cells. High glutaminase and low glutamine synthase activity were reported in many cancer studies (Hirayama et al. 2009; Moreadith and Lehninger 1984). Elevated serum glutamate levels were also observed in prostate cancer and considered as a potential target for cancer treatment (Koochekpour et al. 2012). Glutamate has been reported to promote pancreatic cancer cell invasion and migration (Herner et al. 2011) and brain tumor growth (Takano et al. 2001). Glutamine and glutamate were also shown to be products of TCA cycle activity in a brain tumor ^{13}C NMR study (Maher et al. 2012). We found a strong negative correlation between glucose and glutamate in both *Group 1* ($r = -0.93$) and *Group 3* ($r = -0.95$), consistent with increased TCA cycle activity. The changes in intracellular glutamate and glutamine concentrations were reversed after blocking Y2R with BIIE, especially glutamine. This provided evidence that glutaminolysis was

significantly influenced by NPY activation of Y2R. No correlation was observed between glutamate and glutamine following NPY treatment ($r = 0.01$), however, while glutamate concentrations were negatively correlated with glucose concentrations, glutamine concentrations trended to correlate with glucose concentrations (Table 1), implying that increased glutaminolysis accompanied increased glycolysis, indicating NPY activation of Y2R supported cell proliferation. Glutamine has been considered as an energy source for cancer cells (Hirayama et al. 2009; Medina et al. 1992). So the low intracellular glutamine concentration in NPY-treated cells may indicate increased consumption of glutamine by activated tumor cells. The moderate negative correlation between glutamate and glutamine observed in NPY+BIIE-treated cells (*Group 3*) ($r = -0.61$) may indicate glutamate conversion to glutamine and less glutamine consumption.

Glycine and alanine are also products of glycolysis, so the increase of glycine and alanine in NPY-treated cells may reflect increased glycolysis associated with increased consumption of glucose, and they both were negatively correlated with intracellular glucose in both *Group 1* (alanine −0.72 and glycine −0.96) and *Group 3* (alanine −0.94 and glycine −0.89) which implies they are likely products of glucose consumption and glycolysis. The general relationship of the changes observed in intracellular concentrations of amino acids and the TCA cycle is shown in Fig. 3. The concentrations of alanine, glutamate, glycine, proline, threonine and tyrosine were increased in *Group 1* and decreased in *Group 3*. Increased intracellular concentrations of amino acids in tumors has been suggested to be due to increased autophagic degradation of proteins (Hirayama et al. 2009), and the decreased concentrations of amino acids associated with BIIE blocking of Y2R may be associated with decreased protein degradation.

3.3.3 *O*-Phosphocholine and acetate

Phosphocholine was found to be accumulated in breast cancer cells and has been considered as a biomarker of breast cancer (Eliyahu et al. 2007). The increased *O*-phosphocholine concentrations observed after NPY activation of Y2R was reversed by BIIE treatment, which may imply that NPY activation of Y2R induces choline import to cell. Increased acetate concentrations have been observed in different cancers (Yoshimoto et al. 2001). Though the increase of acetate was not significant in *Group 1* and *Group 2*, the acetate concentration was significantly decreased after adding the BIIE to block Y2R, which may indicate that acetate is related to Y2R activity. Acetate also showed a strong negative correlation with glucose (−0.84) in *Group 3* but a weaker negative correlation in *Group 1* (−0.42). Acetate is related to the TCA cycle by acting as the source of acetyl-CoA, and the relationship between acetate and glucose is linked because of their relative roles in the TCA cycle. High acetate in tumor cells has been considered due to enhanced lipid synthesis (Yoshimoto et al. 2001), so the weaker relationship between acetate and glucose in *Group 1* may be because of its conversion to lipids.

4 Conclusions

The increased expression of NPY and its receptors play an important role in the growth of many human tumors. The NPY Y2R has been found highly expressed in brain tumors and has been considered as a potential target for treatment. In this study, we investigated the metabolic response of human SK-N-BE2 neuroblastoma cells to activation of Y2R with NPY and blocking of Y2R with BIIE. The NPY treatment exhibited dramatic effects on glycolysis, glutaminolysis and TCA cycle activity that were largely abolished by blocking Y2R activity with BIIE. NPY activation of Y2R resulted in changes in cellular metabolism consistent with a Warburg effect. The significant increase of Warburg effect supports the idea that tumor growth is stimulated by NPY activation of Y2R. Intracellular concentrations of many amino acids were increased in response to NPY treatment, which is consistent with previous studies of colon and stomach cancer, and are thought to result from the autophagic degradation of proteins during tumor growth. Though no TCA cycle intermediates were detected, probably due to their low steady-state concentrations inside the cells, the increase of glutamate and its highly correlated relationship with glucose provided evidence of increased TCA activity. Furthermore, our results indicate lower steady-state intracellular nutrient concentrations in cells following Y2R activation by NPY, associated with high glucose conversion to lactate, glycine and alanine. Finally, BIIE appears to effectively and strongly block NPY activation of Y2R supporting its use as a potentially effective treatment to slow human neuroblastoma growth.

Acknowledgments The authors would like to acknowledge support of Miami University and the Ohio Board of Regents for funding to establish the Ohio Eminent Scholar Laboratory. All NMR data collection was conducted at the Ohio Biomedicine Center of Excellence in Structural Biology and Metabonomics at Miami University. We acknowledge Vaib Hebbalalu for his assistance in collecting the NMR data. MAK would also like to acknowledge support from Bruker Biospin, Inc that enabled development of the statistical significance analysis software used in the analysis of the data reported in this paper. This study was supported, in part, by Grants from Shriners Hospital for Children, #86400 and a Department of Veteran Affairs Grant, #1I01BX000263 (AB).

Compliance with ethical requirements This article does not contain any studies with human or animal subjects.

Conflict of interest The authors declare that they have no conflict of interest.

References

Acosta, A., Hurtado, M., Gorbatyuk, O., La Sala, M., Duncan, D., Aslanidi, G., et al. (2011). Salivary PYY: A putative bypass to satiety. *Plos One, 6*(10), e26137.

Aydin, C., Oztan, O., & Isgor, C. (2011). Effects of a selective Y2R antagonist, JNJ-31020028, on nicotine abstinence-related social anxiety-like behavior, neuropeptide Y and corticotropin releasing factor mRNA levels in the novelty-seeking phenotype. *Behavioural Brain Research, 222*, 332–341.

Balasubramaniam, A., Tao, Z., Zhai, W., Stein, M., Sheriff, S., Chance, W. T., et al. (2000). Structure-activity studies including a Psi(CH(2)-NH) scan of peptide YY (PYY) active site, PYY(22-36), for interaction with rat intestinal PYY receptors: Development of analogues with potent in vivo activity in the intestine. *Journal of Medicinal Chemistry, 43*, 3420–3427.

Bensinger, S., & Christofk, H. (2012). New aspects of the Warburg effect in cancer cell biology. *Seminars in Cell & Developmental Biology, 23*, 352–361.

Brothers, S., Saldanha, S., Spicer, T., Cameron, M., Mercer, B., Chase, P., et al. (2010). Selective and brain penetrant neuropeptide Y Y2 receptor antagonists discovered by whole-cell high-throughput screening. *Molecular Pharmacology, 77*, 46–57.

Brothers, S., & Wahlestedt, C. (2010). Therapeutic potential of neuropeptide Y (NPY) receptor ligands. *EMBO Molecular Medicine, 2*, 429–439.

Cabrele, C., & Beck-Sickinger, A. (2000). Molecular characterization of the ligand-receptor interaction of the neuropeptide Y family. *Journal of Peptide Science, 6*, 97–122.

Chronwall, B. M., & Zukowska, Z. (2004). Neuropeptide Y, ubiquitous and elusive. *Peptides, 25*, 359–363.

Dumont, Y., Cadieux, A., Doods, H., Pheng, L. H., Abounader, R., Hamel, E., et al. (2000). BIIE0246, a potent and highly selective non-peptide neuropeptide Y Y(2) receptor antagonist. *British Journal of Pharmacology, 129*, 1075–1088.

Eaton, K., Sallee, F., & Sah, R. (2007). Relevance of neuropeptide Y (NPY) in psychiatry. *Current Topics in Medicinal Chemistry, 7*, 1645–1659.

Eliyahu, G., Kreizman, T., & Degani, H. (2007). Phosphocholine as a biomarker of breast cancer: Molecular and biochemical studies. *International Journal of Cancer, 120*, 1721–1730.

Erlinge, D., Brunkwall, J., & Edvinsson, L. (1994). Neuropeptide Y stimulates proliferation of human vascular smooth muscle cells: Cooperation with noradrenaline and ATP. *Regulatory Peptides, 50*, 259–265.

Gehlert, D. R. (2004). Introduction to the reviews on neuropeptide Y. *Neuropeptides, 38*, 135–140.

Goodpaster, A., & Kennedy, M. (2011). Quantification and statistical significance analysis of group separation in NMR-based metabonomics studies. *Chemometrics and Intelligent Laboratory Systems, 109*, 162–170.

Goodpaster, A., Romick-Rosendale, L., & Kennedy, M. (2010). Statistical significance analysis of nuclear magnetic resonance-based metabonomics data. *Analytical Biochemistry, 401*, 134–143.

Gottschalk, M., Ivanova, G., Collins, D., Eustace, A., O'Connor, R., & Brougham, D. (2008). Metabolomic studies of human lung carcinoma cell lines using in vitro H-1 NMR of whole cells and cellular extracts. *NMR in Biomedicine, 21*, 809–819.

Hansel, D., Eipper, B., & Ronnett, G. (2001). Neuropeptide Y functions as a neuroproliferative factor. *Nature, 410*, 940–944.

Herner, A., Sauliunaite, D., Michalski, C., Erkan, M., De Oliveira, T., Abiatari, I., et al. (2011). Glutamate increases pancreatic cancer cell invasion and migration via AMPA receptor activation and Kras-MAPK signaling. *International Journal of Cancer, 129*, 2349–2359.

Hirayama, A., Kami, K., Sugimoto, M., Sugawara, M., Toki, N., Onozuka, H., et al. (2009). Quantitative metabolome profiling of colon and stomach cancer microenvironment by capillary electrophoresis time-of-flight mass spectrometry. *Cancer Research, 69*, 4918–4925.

Ingenhoven, N., & Beck-Sickinger, A. (1999). Molecular characterization of the ligand-receptor interaction of neuropeptide Y. *Current Medicinal Chemistry, 6*, 1055–1066.

Kitlinska, J., Abe, K., Kuo, L., Pons, J., Yu, M., Li, L., et al. (2005). Differential effects of neuropeptide Y on the growth and vascularization of neural crest-derived tumors. *Cancer Research, 65*, 1719–1728.

Koochekpour, S., Majumdar, S., Azabdaftari, G., Attwood, K., Scioneaux, R., Subramani, D., et al. (2012). Serum glutamate levels correlate with gleason score and glutamate blockade decreases proliferation, migration, and invasion and induces apoptosis in prostate cancer cells. *Clinical Cancer Research, 18*, 5888–5901.

Korner, M., & Reubi, J. (2007). NPY receptors in human cancer: A review of current knowledge. *Peptides, 28*, 419–425.

Korner, M., & Reubi, J. (2008). Neuropeptide Y receptors in primary human brain tumors: Overexpression in high-grade tumors. *Journal of Neuropathology and Experimental Neurology, 67*, 741–749.

Korner, M., Waser, B., & Reubi, J. (2004). High expression of neuropeptide Y receptors in tumors of the human adrenal gland and extra-adrenal paraganglia. *Clinical Cancer Research, 10*, 8426–8433.

Kruskal, W. H., & Wallis, W. A. (1952). Use of ranks in one-criterion variance analysis. *Journal of the American Statistical Association, 47*, 583–621.

Lee, E., Grant, D., Movafagh, S., & Zukowska, Z. (2003). Impaired angiogenesis in neuropeptide Y (NPY)-Y2 receptor knockout mice. *Peptides, 24*, 99–106.

Lindon, J. C., Nicholson, J. K., & Holmes, E. (2007). *The Handbook of Metabonomics*. The Handbook of Metabonomics: Elsevier.

Lu, C., Everhart, L., Tilan, J., Kuo, L., Sun, C., Munivenkatappa, R., et al. (2010). Neuropeptide Y and its Y2 receptor: Potential targets in neuroblastoma therapy. *Oncogene, 29*, 5630–5642.

Maher, E., Marin-Valencia, I., Bachoo, R., Mashimo, T., Raisanen, J., Hatanpaa, K., et al. (2012). Metabolism of [U-13C] glucose in human brain tumors in vivo. *NMR in Biomedicine, 25*, 1234–1244.

Medeiros, P., Al-Khazraji, B., Novielli, N., Postovit, L., Chambers, A., & Jackson, D. (2012). Neuropeptide Y stimulates proliferation and migration in the 4T1 breast cancer cell line. *International Journal of Cancer, 131*, 276–286.

Medeiros, P., & Jackson, D. (2013). Neuropeptide Y Y5-receptor activation on breast cancer cells acts as a paracrine system that stimulates VEGF expression and secretion to promote angiogenesis. *Peptides, 48*, 106–113.

Medina, M. A., Sanchez-Jimenez, F., Marquez, J., Rodriguez Quesada, A., & Nunez de Castro, I. (1992). Relevance of glutamine metabolism to tumor cell growth. *Molecular and Cellular Biochemistry, 113*, 1–15.

Moreadith, R. W., & Lehninger, A. L. (1984). The pathways of glutamate and glutamine oxidation by tumor cell mitochondria. Role of mitochondrial NAD(P)+-dependent malic enzyme. *The Journal of biological chemistry, 259*, 6215–6221.

Movafagh, S., Hobson, J., Spiegel, S., Kleinman, H., & Zukowska, Z. (2006). Neuropeptide Y induces migration, proliferation, and tube formation of endothelial cells bimodally via Y1, Y2, and Y5 receptors. *Faseb Journal, 20*, 1924–1926.

O'Donohue, T. L., Chronwall, B. M., Pruss, R. M., Mezey, E., Kiss, J. Z., Eiden, L. E., et al. (1985). Neuropeptide Y and peptide YY neuronal and endocrine systems. *Peptides, 6*, 755–768.

Park, I., Larson, P. E. Z., Zierhut, M. L., Hu, S., Bok, R., Ozawa, T., et al. (2010). Hyperpolarized 13C magnetic resonance metabolic imaging: Application to brain tumors. *Neuro-Oncology, 12*, 133–144.

Reubi, J., Gugger, M., Waser, B., & Schaer, J. (2001). Y-1-mediated effect of neuropeptide Y in cancer: Breast carcinomas as targets. *Cancer Research, 61*, 4636–4641.

Ruscica, M., Dozio, E., Motta, M., & Magni, P. (2007). Relevance of the neuropeptide Y system in the biology of cancer progression. *Current Topics in Medicinal Chemistry, 7*, 1682–1691.

Sheriff, S., Ali, M., Yahya, A., Haider, K., Balasubramaniam, A., & Amlal, H. (2010). Neuropeptide Y Y5 receptor promotes cell growth through extracellular signal-regulated kinase signaling and cyclic amp inhibition in a human breast cancer cell line. *Molecular Cancer Research, 8*, 604–614.

Simes, R. J. (1986). An improved Bonferroni procedure for multiple tests of significance. *Biometrika, 73*, 751–754.

Smialowska, M., Domin, H., Zieba, B., Kozniewska, E., Michalik, R., Piotrowski, P., & Kajta, M. (2009). Neuroprotective effects of neuropeptide Y-Y2 and Y5 receptor agonists in vitro and in vivo. *Neuropeptides, 43*, 235–249.

Takano, T., Lin, J., Arcuino, G., Gao, Q., Yang, J., & Nedergaard, M. (2001). Glutamate release promotes growth of malignant gliomas. *Nature Medicine, 7*, 1010–1015.

Tatemoto, K., Carlquist, M., & Mutt, V. (1982). Neuropeptide Y—a novel brain peptide with structural similarities to peptide YY and pancreatic polypeptide. *Nature, 296*, 659–660.

van den Berg, R., Hoefsloot, H., Westerhuis, J., Smilde, A., & van der Werf, M. (2006). Centering, scaling, and transformations: Improving the biological information content of metabolomics data. *BMC Genomics, 7*, 142.

Wang, B., Shi, Z., Weber, G., & Kennedy, M. (2013). Introduction of a new critical p value correction method for statistical significance analysis of metabonomics data. *Analytical and Bioanalytical Chemistry, 405*, 8419–8429.

Watanabe, M., Sheriff, S., Kadeer, N., Cho, J., Lewis, K., Balasubramaniam, A., & Kennedy, M. (2012). NMR based metabonomics study of NPY Y5 receptor activation in BT-549, a human breast carcinoma cell line. *Metabolomics, 8*, 854–868.

Wu, P., & Otting, G. (2005). Rapid pulse length determination in high-resolution NMR. *Journal of Magnetic Resonance, 176*, 115–119.

Yoshimoto, M., Waki, A., Yonekura, Y., Sadato, N., Murata, T., Omata, N., et al. (2001). Characterization of acetate metabolism in tumor cells in relation to cell proliferation: Acetate metabolism in tumor cells. *Nuclear Medicine and Biology, 28*, 117–122.

Zhang, L., Bijker, M., & Herzog, H. (2011). The neuropeptide Y system: Pathophysiological and therapeutic implications in obesity and cancer. *Pharmacology and Therapeutics, 131*, 91–113.

Zhang, S., Zheng, C., Lanza, I., Nair, K., Raftery, D., & Vitek, O. (2009). Interdependence of signal processing and analysis of urine H-1 NMR Spectra for Metabolic Profiling. *Analytical Chemistry, 81*, 6080–6088.